PRECISION ULTRASONIC THICKNESS MEASUREMENTS OF THIN STEEL DISKS

G.V. Blessing, D.G. Eitzen, and J.F. Henning

National Bureau of Standards
Gaitherberg, MD 20899

A.V. Clark, Jr. and R.E.Schramm

National Bureau of Standards
Boulder,CO 80303

INTRODUCTION

The accurate in-situ measurement of part dimensions during fabrication is of much interest to the manufacturing industry, especially for untended manufacturing. The goal of this work is to apply non-contacting ultrasonic techniques to the precise thickness measurement, during machining, of metal parts of rotation having a nominal wall thickness of 1.5 mm. The desired accuracy is ± .0025 mm at all points on the approximately 200 mm diameter steel shells, where part access is restricted to one side at a time for the measurement. In a feasibility study, dimensional information using eddy current techniques was overwhelmed by conductivity variations in the 304-stainless steel samples [1]. The approach here is to precisely measure ultrasonic echo transit times, and calulate part dimensions, knowing the material sound speed. To that end, feasibility results on flat disk specimens possessing a wide range of grain sizes representative of the shell's variable metallurgy are reported here. Factors affecting ultrasonic dimensional precision including grain size, texture, sample temperature and surface roughness are discussed, with an emphasis on precision limitations due to finite grain sizes in thin parts. Both longitudinal (10 to 30 MHz) and shear (3 MHz) wave measurements were made, the latter using electromagnetic acoustic transducers (EMATS). Finally, comparisons were made of the ultrasonic dimensional values with precision interferometer measurements.

APPROACH

Ultrasonic transit-time measurements of longitudinal (compressional) wave pulses were made on well-characterized sample disks to determine the limitations of various material parameters for ultrasonic dimensional precision. The samples were characterized for grain size, homogeneity, surface roughness, and thickness. The expectation is that a meaningful value for the material sound velocity V can be determined to link the measured transit times t to the sample dimension D:

$$D = V*t. \qquad (1)$$

A grand average <V> of all sample velocities was chosen to be this proportionality constant. Its variation within samples was the principal limitation to ultrasonic dimensional precision.

A second approach, with shear waves, was to make relative dimensional measurements using a resonant-thickness technique. Knowing the sample thickness at a reference point, dimensional changes were measured by monitoring the phase change of the resonant wave form as the sample was scanned.

EXPERIMENTAL

Ultrasonic Techniques

Longitudinal wave transit-time precision was evaluated as a function of ultrasonic wave frequency for the variable grain-size samples representing the range of metallurgical conditions expected in the 304-stainless steel shells. A manual pulse-echo-overlap broadband immersion technique [2] was used for wave pulses with peak frequencies ranging from 10 to 30 MHz. Focused and unfocused piezoelectric ceramic tranducers were operated at their respective far-field distances with a liquid (varsol or water) delay line. Multiple sample echoes, six when possible, were used to increase measurement precision of the transit time. The ultrasonic instrumentation consisted of a crystal-based time-interval averaging system in conjunction with an oscilloscope time delay feature having a resolution of 0.1 ns, and a broadband shock excitation pulser/receiver unit. Pulse-echo-overlap measurement precision was nominally 1.0 ns or better, depending on sample grain size which in turn affected the number of useful sample echoes. From eq. (1), a 1.0 ns precision yields a thickness precision of about 0.5 μm assuming six sample echoes and a V = 5.8 mm/μs. This is a conservative estimate of the system capability at 10 MHz since the observed precision of the majority of data was 0.2 to 0.3 ns, implying a dimensional precision approaching 0.1 μm assuming V is precisely known.

Shear wave time measurements were made to (a) corroborate the longitudinal wave data, and (b) to enable the consideration of a velocity combinations approach [3] to minimize or eliminate velocity variations due to material texture. The approach would take advantage of the following invariant relationship for cubic crystallites:

$$\Sigma_j \, V_j^2 = \frac{1}{\rho} \, (C_{11} + 2C_{44}), \qquad (2)$$

where V_j represents one longitudinal and two shear modes with particle motions along the three principal axes of (unidirectional) rolled extruded material, ρ is the density, and the C_{ij} are second order elastic coefficients for a cubic system. Having independently established the constant quantity on the right-hand-side, the thickness dimension may be determined from three separate transit-time measurements. While in general the propagation of errors may limit the usefulness of this approach, it may prove of value for highly textured materials.

Shear wave relative time measurements were made using a resonant thickness technique near 3 MHz, driving the thin disk sample at its third harmonic by matching 3/2 λ to the thickness. A nominally ten cycle duration driving pulse was applied to an EMAT of one square centimeter aperture. The phase of the sensed resonant vibration was monitored up to 100 μs later with a precision of about 5 ns, yielding a dimensional precision comparable to that of the longitudinal wave technique. In addition, a limited set of shear wave broadband transit-time measurements were made by pulse-echo-overlap using a direct-contact dry coupling technique.

Samples

Four flat disk samples were sliced from 75 mm diameter hot-rolled bar to a thickness of 1.5 mm. Two disks possessed a similar fine-grain structure, while the other two were subsequently heat treated to form a varied coarse-grain structure. Using ASTM grain size nomenclature [4], the grains ranged from No. 3 to No. 7, representing a respective nominal dimensional range of 150 to 30 μm. An interferometer-based contacting comparator system provided thickness data at eight discrete points across an arbitrary diameter of each sample, accurate to about 0.1 μm [5]. Sample thickness varied as much as 65 μm, monotonically decreasing from center to edge for all samples. The average surface roughness values determined with a contacting stylus were less than 0.5 μm. However, the 1 μm roughness values measured at a couple of surface locations could conflict with the desired $\pm$ 2.5 μm thickness accuracy. For example, an average roughness value R_a of only 1 μm can result from peak to valley sinusoidal surface excursions of nearly 3 μm [6]. If such apparently innocuous surface features were on both sides of the part, the resulting statistical fluctuations in part thickness could be problematic. Front-surface echo amplitude scans at 20 MHz (75 μm ultrasonic wavelength in water) were in fact sensitive to particular regions of the samples' surfaces.

Ultrasonic Variables

The scattered-wave profiles of back-surface echo amplitude scans provided a measure of sample homogeneity. At 20 MHz, the 0.3 mm wavelength probe in steel was very sensitive to the coarser-grain samples with grains $\geq$ 0.1 mm. Of greater signifcance for the purpose of this work, however, was the direct effect of the samples' polycrystalline nature on the velocity and therefore on dimensional measurement precision. Both large grains and grain alignment can inhibit ultrasonic dimensional precision. Even in a random aggregate, large grains (relative to the ultrasonic path length) can lead to significant velocity variations, i.e. elastic inhomogeneity. This is to be distinguished from a non-random orientation or alignment of grains (whether large or small) that results in texturing and elasic anisotropy.

Based on model calculations by Mason and McSkimin [7] and by Stanke [8] respectively for longitudinal and shear wave propagation in polycrystalline aggregates, Fisher and Johnson [9] have recently pointed out the substantial velocity variations that can be expected in metals. The model, based on the statistical stacking distribution of N randomly oriented crystallites in the ultrasonic path, assumes the average aggregate velocity is equal to the average single crystal velocity. The model may be simply stated mathmatically as:

$$V = V_o \pm \Delta V(N), \tag{3}$$

where V_o is the average velocity and ΔV is the measured velocities' statistical fluctuation which decreases as N increases. Applying the central limit theorem in statistics which states that for sufficiently large N, V is a random variable whose variance S^2 is proportional to the single crystal variance S_o^2 and inversely proportional to N:

$$S^2 = S_o^2/N. \tag{4}$$

The constant S_o^2 depends on whether the wave propagation is longitudinal or shear. For randomly oriented crystals of cubic structure, the normalized

standard deviations (S_o) for longitudinal [7] and shear [8] waves, in terms of the elasic coefficients, are respectively:

$$S_{o\ell} = \frac{2}{5\sqrt{21}} \frac{\mu}{C_{12} + C_{44} - 2\mu/5}, \quad (5)$$

$$S_{os} = \frac{1}{10} \sqrt{\frac{2}{3}} \frac{\mu}{C_{44} + \mu/5}, \quad (6)$$

where $\mu = (C_{11} - C_{12} - 2C_{44})$ is the anisotropy term. A lesser crystalline anisotropy and/or smaller crystals reduces the velocity variance in a sample of given thickness. Based on these models, an analysis of the longitudinal wave variance that can be expected for our stainless samples is given under Results.

The second principal area of consideration for polycrystalline effects on the velocity is texturing caused by grain alignment during material processing. Much work has been done to elucidate and quantify this effect in terms of readily measured sound velocities [3]. The basic relationship may be stated as:

$$V = V_o + f(W_{\alpha\beta\gamma}) \quad (7)$$

where V_o is the velocity without texture, and the crystal orientation distribution coefficients $W_{\alpha\beta\gamma}$ define the level of sample texture. The three first order $W_{\alpha\beta\gamma}$ pertinent to a cubic grain structure are determined by propagating different wave modes in specific directions relative to the principal material axes. While the necessary measurements have not been made for a complete texture analysis, shear wave measurements indicated that at least the in-plane anisotropy (proportional to W_{420}) was not significant.

Thermal effects on dimensional precision were evaluated. The sample temperature affects the material elasticity and therefore sound velocity [10]. Thermal expansion and contraction also occurs, but based on handbook-value calculations, the effect is several orders of magnitude less than that on the elasticity, and is therefore neglected here. For small changes of temperature T:

$$V = V_o\ (T_o) + \alpha\Delta T, \quad (8)$$

where V_o is the velocity at room temperature, T_o, and α is a material dependent constant. For our 304-stainless samples, α was -1.5×10^{-3} mm/μs/°C between 18 and 23°C. For the intended temperature tolerance of 20 ± 0.5°C during part fabrication and measurement, the resulting velocity variation would be ± 1/8000 or less than 10% of the error budget. This contribution to the uncertainty could be made negligible in practice by referencing transit times on-line to a sample at the same temperature as the part being measured.

RESULTS

Longitudinal Waves

Transit-time measurements were made on all four disks using broadband transducers with peak frequencies of 10, 20, and 30 MHz. Based on criteria of reproducibility and accuracy for the entire range of grain-size material, optimum results were obtained at 10 MHz. Measurement reproducibility was observed to generally decrease with increasing frequency. This was the case for even the finer grain samples where the average standard deviation

increased sixfold between 10 and 30 MHz based on a set of three repeated measurements at each sample position. Besides reducing the number of useful sample echoes at 20 and 30 MHz, the highly attenuating coarser-grain material reduced the echo peak frequencies to less than 20 MHz, obviating the higher frequency measurements. Furthermore, the discrepancy between the ultrasonic values and actual dimensions increased noticeably and randomly at 30 MHz on the coarsest-grain sample. (The lateral focal regions of the 10 and 30 MHz transducers were respectively 2.0 and 0.4 mm diameter at half amplitude in water.) These observations are attributed to three principal effects. Increasing the ultrasonic frequency (i) reduced the wavelength to grain size ratio which increased wave scattering, (ii) led to reduced beam apertures which in turn reduced the number of grains to be sampled and averaged within the ultrasonic path, and (iii) due to both the smaller wavelength and beam aperture, increased measurement sensitivity to repositioning and angulation.

Recognizing the material sound velocity in eq. (1) as a significant variable affecting ultrasonic dimensional precision, it is plotted as a function of position along arbitrarily chosen diameters of all four disks in Fig. 1. Sample temperature was kept constant to ± 0.1°C during all measurements. Each data point is the comparator dimensional value divided by the average of three transit-time measurements. The transit-time measurements were quite repeatable; if error bars representing repeatability were included in Fig. 1, they would be smaller than the size of the data symbols at all locations but three on the coarse grain material. The uncertainty of the comparator data was negligible on the scale of Fig. 1.

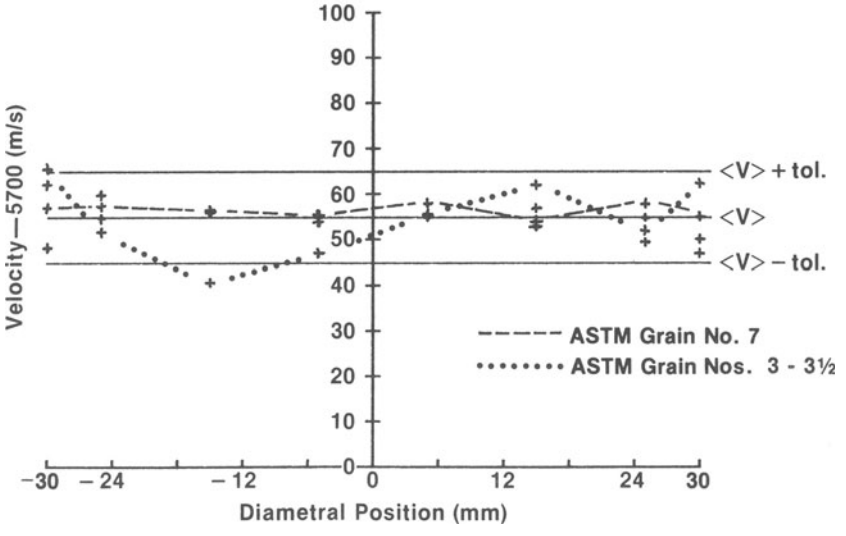

Fig. 1. Ultrasonic longitudinal velocities (+) at eight diametral positions of each of four sample disks. The solid center line is the average of all velocity data, and the solid ± tolerance lines represent extremum acceptable velocity variations. The dashed and dotted lines respectively connect the data for a fine and a coarse grain sample.

The solid center line represents a grand average velocity value <V> of all data on the four disks. The average velocities on individual disks were in fact nearly equal. The upper and lower solid lines represent tolerance bounds if the entire ± 1/600 dimensional error budget pertaining to eq. (1) could be attributed to velocity variations. These bounds very nearly coincide with the two sigma (standard deviation) levels containing 95% of the data distribution. The connecting dashed and dotted lines illustrate the velocity variations observed respectively on a fine-grain (ASTM 7) and on a coarse-grain (ASTM 3-3½) sample.

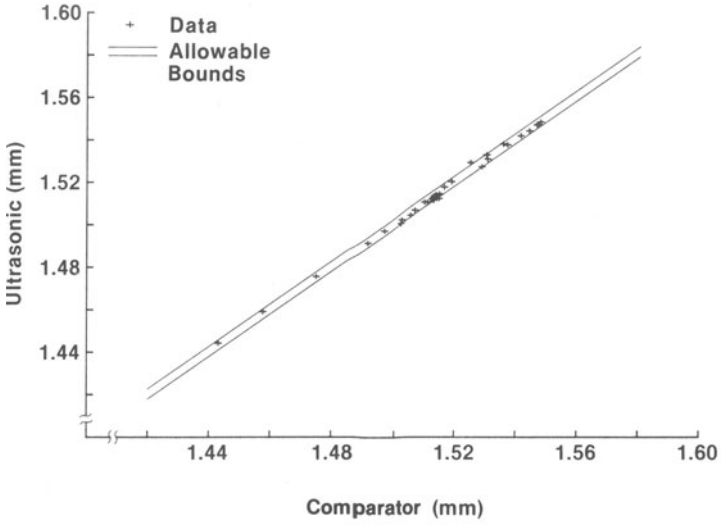

Fig. 2. Ultrasonic versus comparator dimensional data on four sample disks at 10 MHz longitudinal. The pair of solid lines represent the ± 2.5 μm bounds of desired accuracy for the ultrasonic data.

Figure 2 compares the ultrasonic with the comparator dimensional data for all disks. Each ultrasonic value was calculated using the grand average velocity <V> = 5.755 for V in eq. (1). The pair of solid lines represent the allowable bounds of ± 2.5 μm for the desired accuracy. Two of the thirty two data points fell outside these bounds, both of which were in coarse-grain material. If vertical error bars were plotted representing ultrasonic precision in Fig. 2, they would be less than the size of the plotted symbols for all data with the exception of two points where they would be about twice the symbol dimension. Horizontal error bars representing interferometer precision would be negligible.

Figure 3 presents the model contribution of finite grain sizes to the longitudinal velocity variation observed in the four sample disks. The sample standard deviation S of each disk's velocities (over regions of constant grain size) was calculated. These values were normalized to the average velocity $\langle V_L \rangle$ and plotted versus grain size as the solid circles in Fig. 3. The theoretical contribution of grain size to the observed deviation S was calculated from eq. (5) in the model above, using 304-stainless C_{ij} values from Ledbetter [11], and plotted as the solid line. A trend of qualitative agreement may be observed. It is noted that besides grain size, all other material variables including texture, residual stress, and surface roughness may contribute to the experimental deviation, in addition to measurement imprecision. As a result, the solid line may be considered to represent the lower limit of velocity variations that may be expected in practice (due to finite grains), and the shaded region to be a region of dimensional accuracy inaccessible to our ultrasonic measurements.

Shear Waves

Relative shear wave time measurements were also made on the set of four sample disks using a resonant-thickness technique with an EMAT near 3 MHz. Based on an arbitrarily chosen phase point t_o at a zero-crossing in the resonant wave train some 50 to 100 μs after the excitation pulse (corresponding to an ultrasonic path length D_o), the relative dimensional changes δD may be calculated from the measured phase changes δt using the following relationship:

$$\frac{\delta D}{D_o} = \frac{\delta t}{t_o}. \qquad (9)$$

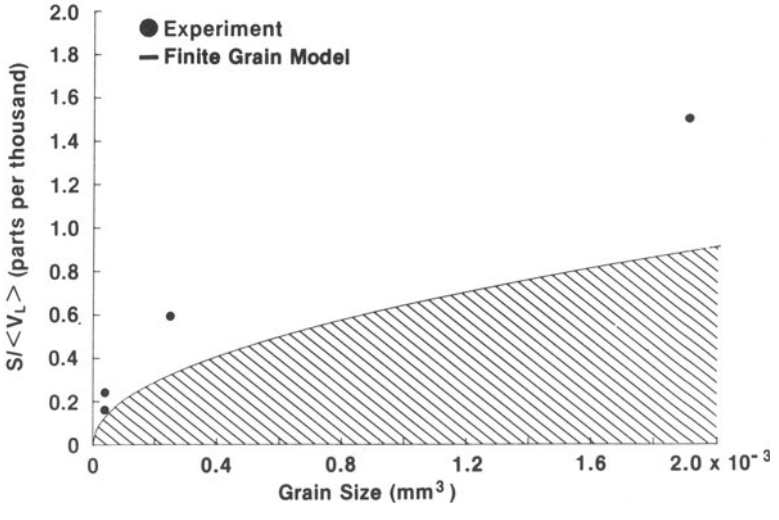

Fig. 3. Statistical longitudinal velocity variations (normalized to the average sound velocity), experimentally observed on four sample disks, versus grain size; and model calculations for the contribution of finite grain size to the observed variations.

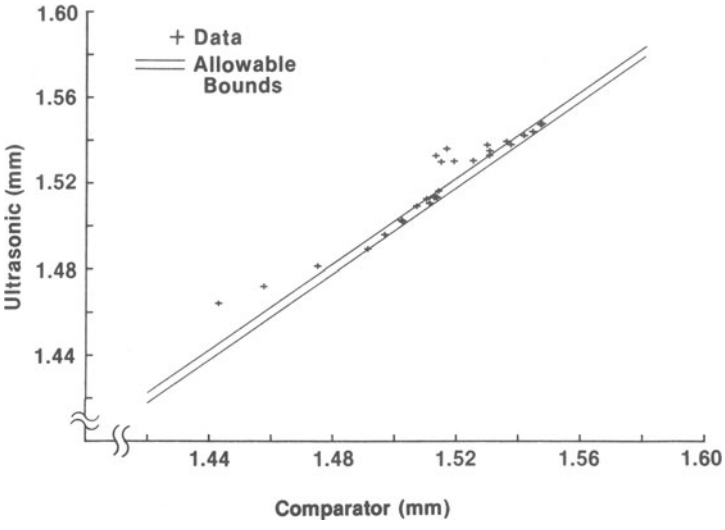

Fig. 4. Ultrasonic versus comparator dimensional data on four sample disks at 3MHz shear. The pair of solid lines represent the ± 2.5 μm bounds of desired accuracy for the ultrasonic data

The absolute dimensions D were calculated and plotted in Fig. 4 similarly to the longitudinal data of Fig. 2. It is noted that all out-of-bounds data was due to large ultrasonic values. Also noted is that the two groupings of high-valued data were obtained on the two coarse-grain samples, whereas the data on the fine-grain samples fell within the ± 2.5 μm bounds. However, upon correlating the observed deviations with sample thickness variations, it became apparent that there were other significant factors affecting ultrasonic precision, including transducer proximity to the sample boundary, and sample surface non-parallelism. (Grain size effects by themselves could not be expected to cause a systematic shift in the data.) Dampening the disk edge by finger pressure noticeably altered the echo profile, indicating possible phase interference by a portion of the resonant echo train reflecting from the sample boundary. Wedge effects [12] were observed by a perturbation of the echo amplitude profile from exponential decay in the regions of non-parallelism. Apparently the resulting increase in path length due to non-normal reflection caused a systematic shift to higher values of δt and therefore of D.

Other sources of shear wave error using the resonant technique should be mentioned, but were judged insignificant by comparison to the effects of sample non-parallelism. The systematic shift in relative dimensional values that can result by referencing phase changes to a single arbitrary sample position D_o at its velocity V_o must be recognized, as well as the effect of grain size based on eqs. (4) and (6). While the calculated value for S_{os} was over four times that for $S_{o\ell}$ in steel, the significantly larger EMAT aperature (than that for the longitudinal wave transducer) should offset the larger S_{os}^2 by a proportionally larger number N of grains sampled (see eq. (4)). Data obtained on one of the samples using a non-resonant direct-contact shear wave technique with short wave pulses substantiated these conjectures by falling within the ± 2.5 μm bounds. Finally, it is noted that neither the data in Fig. 4 nor that obtained by direct contact were significantly affected by rotating the direction of shear polarization.

CONCLUSIONS

Encouraging ultrasonic dimensional measurement results were obtained on flat 1.5 mm thick samples with a range of metallurgical properties by meeasuring 10 MHz (and higher frequency) longitudinal wave transit times in samples immersed in a liquid bath. The ultrasonic values, derived from the product of the transit times and the average material velocity, agreed within ± 2.5 μm of precise comparator measurements at nearly all sample positions.

Among the many material elastic variables considered for their effect on ultrasonic measurement precision, the effect of grain size on the ultrasonic velocity was observed to be the most significant for the longitudinal wave measurements. Relative-phase resonant-thickness shear wave time measurements using a non-contacting EMAT at 3 MHz gave encouraging results in some cases, but resulted in significant error on non-parallel-faced sample regions. Working at a higher ultrasonic frequency to enable absolute transit-time measurements of short duration pulses (as was done for longitudinal waves) would alleviate this problem.

In future applications to thin curved (hemispherical) parts, more attention will need to be given to the effects of variable thickness, the texture of spin-formed shells, and transducer positioning and orientation relative to the surface. For on-line applications, effort will be required to automate the transit-time measurements for rapid data acquisition. In the case of longitudinal waves, efficient coupling of the ultrasound to the part will be required. It is planned to use the cutting fluid in which the part is already bathed, to form a coupling stream.

ACKNOWLEDGEMENT

The authors wish to acknowledge the support of Rockwell International, North American Space Operations, the Rocky Flats Plant, Golden, Colorado.

REFERENCES

1. J.C. Moulder, (private communication) National Bureau of Standards, Boulder, CO. Present address: Center for NDE, Iowa State University, Ames, IA.
2. E.P. Papadakis, in Physical Acoustics, eds. W.P. Mason and R.N. Thurston (Academic Press, NY, 1976) Vol. XII, Chap. 5, pp. 279-298.
3. C.M. Sayers, J. Phys. D (Appl. Phys.) 15 (1982) pp. 2157-2167.
4. Anon. in 1986 Annual Book of ASTM Standards (ASTM, Philadelphia, PA, 1986) Recommended Practices E112 and A262 respectively in Vols. 3.01 and 3.02.
5. T.D. Doiron, (private communication) Precision Eng. Div., National Bureau of Standards, Gaithersburg, MD.
6. Anon. ASME/ANSI B46.1-1985, Surface Texture Waviness and Lay (ASME, NY, 1985).
7. W.P. Mason and H.J. McSkimin, J. Acoust. Soc. Am. 19, No. 3 (1947) pp. 464-473.
8. F.E. Stanke, in Unified Theory and Measurements of Elastic Waves in Polycrystalline Materials, Ph.D dissertation, Stanford University (1983).
9. M.J. Fisher and G.C. Johnson, in Review of Progress in Quantitative NDE, edited by D.O. Thompson and D.E. Chimenti (Plenum Press, NY, 1984) pp. 1119-1128.

10. R. Truell, C. Elbaum, B. Chick, Ultrasonic Methods in Solid State Physics, (Academic Press, NY, 1969) Chap. 2, p. 123.
11. H.M. Ledbetter, Physica 128B (1985) pp. 1-4.
12. R. Truell, C. Elbaum, B. Chick, Ultrasonic Methods in Solid State Physics, (Academic Press, NY, 1969) Chap. 2, p. 107.